PIV and OH PLIF study of impinging propane-air jet-flames

Z D Kravtsov[1,2], Z D Tolstoguzov[1,2], L M Chikishev[1,2], V M Dulin[1,2]

[1]Kutateladze Institute of Thermophysics, Siberian Branch of RAS, 1 Ak. Lavrentyeva Avenue, Novosibirsk, 630090, Russia
[2]Novosibirsk State University, 2 Pirogova Street, Novosibirsk, 630090, Russia

E-mail: l.chikishev@gmail.com

Abstract. The paper reports on the study of flow structure of a reacting propane-air jet, issued from contraction nozzle and impinged on flat metallic surface, by using the particle image velocimetry technique. Flows with different nozzle-to-surface distance H/d were studied. The Reynolds number Re was in the range of 500÷5500, equivalence ratio Φ was varied from 0.8 to 1.4. Velocity field was measured for a conical premixed flame for Re = 1500 and Φ = 0.9. A region with flow recirculation was detected between the flame cone and the impingement surface for the case of H/d = 4. This flow feature may result in a reduced local heat transfer.

1. Introduction

The problem of heat and mass transfer during cooling and heating of surfaces by jet flows is relevant for a number of technical applications (e.g., paper drying, glass heating, cooling of microelectronics or turbine blades). One of the major shortcomings in the organization of impinging isothermal and reacting flows is the heterogeneity of the local heat transfer. Some applications, such as chemical vapor deposition, require homogeneity of heat and mass transfer. Vortex structures rolling-up in shear layer of jet flows influence on local heat transfer for small distances between the nozzle and surface [1-4]. Manipulation by these vortices (e.g., by external forcing) can be used to affect local intensity of heat transfer. Particle image velocimetry (PIV) and planar laser-induced fluorescence (PLIF) are useful tools to investigate influence of unsteady flow structures on heat transfer in impinging jets [5]. In impinging jets with premixed combustion, self-induced instabilities can arise without external forcing [6, 7]. Influence of this factor on heat transfer requires further studies.

Besides, near-wall combustion phenomena influence on the efficiency and formation of pollutions in many technical applications. This aspect is of a growing interest for modern downsized internal combustion engines with increased surface-to-volume ratios and higher power densities. Furthermore flame-wall interactions also affect the combustion in jet engines and gas turbine combustors. Since flame-wall interaction processes are not yet understood in details, the complex interactions between fluid motion, transport phenomena and chemical reactions during these processes need further investigations. Experimental studies of near-wall combustion in simplified geometry are required.

The present work focuses on PIV/PLIF measurements in a reacting jet, interacting with a flat wall in a simplified geometry. Namely, a conical premixed flame covered from the top with a flat water-cooled surface is studied. The confinement effect on the flow pattern has been investigated.

2. Apparatus and setup

The reacting jet flow of propane-air mixture issued from a contraction axisymmetric nozzle (with the outlet diameter d of 15 mm). The jet impinged normally on flat surface of the bottom of water-cooled

cylindrical tank. The axis of the cylinder was aligned with the nozzle axis. The cylinder diameter was 80 mm. An electric traversing device was used to move the tank along its axis with the precision of 0.1 mm. The scheme of the experimental setup is shown in Figure1. A lighter was used to ignite the flame.

Flow rates of the air and propane were controlled by flow meters. The details about the burner can be found in the previous study [8]. Titanium dioxide particles of approximately 0.5 μm in diameter were used to seed the flow for the PIV measurements. The particles were contained in a vessel and were introduced to the passing through air flow by a mechanical mixer. The vessel was connected to the air supply line via a bypass scheme.

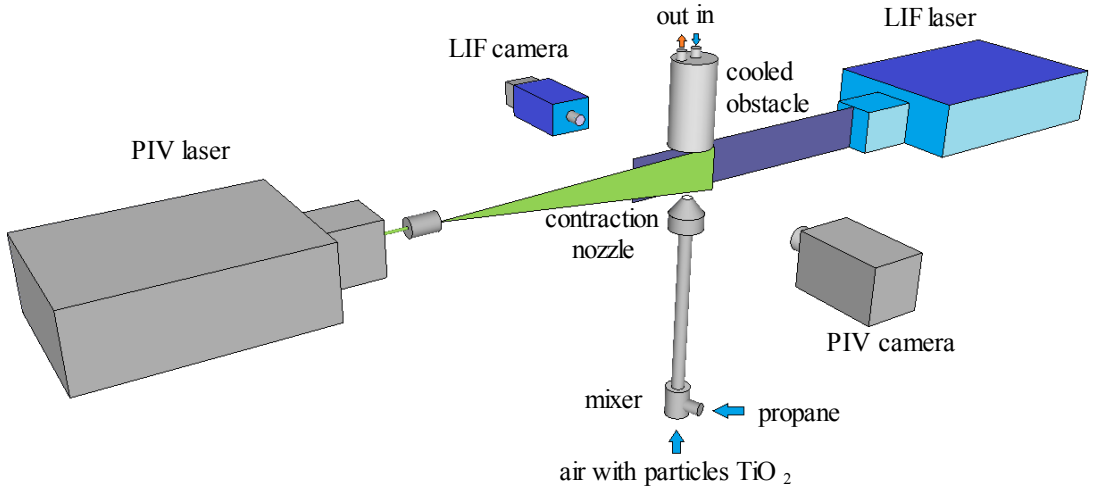

Figure 1. Sketch of PIV/PLIF experimental setup

Particle image velocimetry (PIV) was used for the measurement of velocity fields. Measuring area size was 80×80 mm. Double-head Nd:YAG laser (Quantel, Ever Green, up to 70mJ per each 7 ns pulse) was used to illuminate the particles in the measurement plane. The laser beam was converted into a laser sheet by using a system of cylindrical and spherical lenses. The opening angle of the laser sheet was 10 degrees. The energy of each laser pulse was measured by a power meter (Coherent LabMax). On average it was 53 mJ after the laser sheet optics.

Particles images were captured by a CCD camera (Bobcat ImperX), oriented normally to the laser sheet plane. A narrow band-pass optical filter (532 nm ± 10 nm) was used to reduce intensity of background and flame luminosity in the camera image. The laser and camera were synchronized via TTL signal. The time delay between two pulses for each image pair was 100 μs and corresponded to maximal displacement of the particles up to 15 pixels. The PIV images (2048×2048 pixels is size) were processed by using in-house software ActualFlow. The images were preprocessed to remove background (minimal intensity for each pixel) and impingement surface. During four iterations of an adaptive cross-correlation algorithm the interrogation area size was reduced from 64×64 to 32×32 pixels. The spatial overlap rate between the interrogation areas was 50%. The velocity fields were validated by signal-to-noise criterion.

A PLIF system (LaVision) was used to measure temperature distribution in the longitudinal cross-section of the jet-flame from OH* fluorescence. The second harmonic (532 nm) of a pulsed Nd:YAG laser (Quanta-Ray, 10Hz, 1 J per pulse) was used to pump a tunable dye laser (Sirah dye laser) with Rhodamine 6G. Frequency of the output radiation was doubled by using a BBO crystal. A small portion of the laser radiation was directed to a power meter using a semi-transparent mirror. The measurement of the energy of each laser pulse was necessary for correct comparison of the instantaneous fluorescence images with each other. The energy of the laser radiation in the wavelength range 283-284 nm was approximately 10 mJ. The laser beam was transformed into a collimated sheet

with a width of 50 mm and thickness less than 0.8 mm (in the measurement region). The laser sheet passed through the axis of symmetry of the nozzle.

Image intensifier (LaVision IRO) based on a UV-sensitive photocathode S20 (multialkali) and multi-channel amplifier, was used to register fluorescence signal of the OH*. The quantum efficiency of the photocathode was about 25% for the considered wavelength range (280-320 nm). The image intensifier was equipped with a quartz lens (LaVision UV-lens, f # 2.8, 100 mm) and optical band-pass filter (300-320 nm). The use of the optical filter was necessary to remove unwanted intensity at the wavelength of the lasers, including reflections by the nozzle. The signal was recorded by sCMOS camera (16-bit images with resolution of 2560 × 2160 pixels). The images were processed by FlameMaster software from LaVision.

3. Results and discussion

3.1. PIV and PLIF data for unconfined flame

Temperature of the combustion products were detected by comparing intensity of OH* fluorescence, excited by two different transitions.

Figure 2. Examples of OH* PLIF intensity during excitation of two different transitions

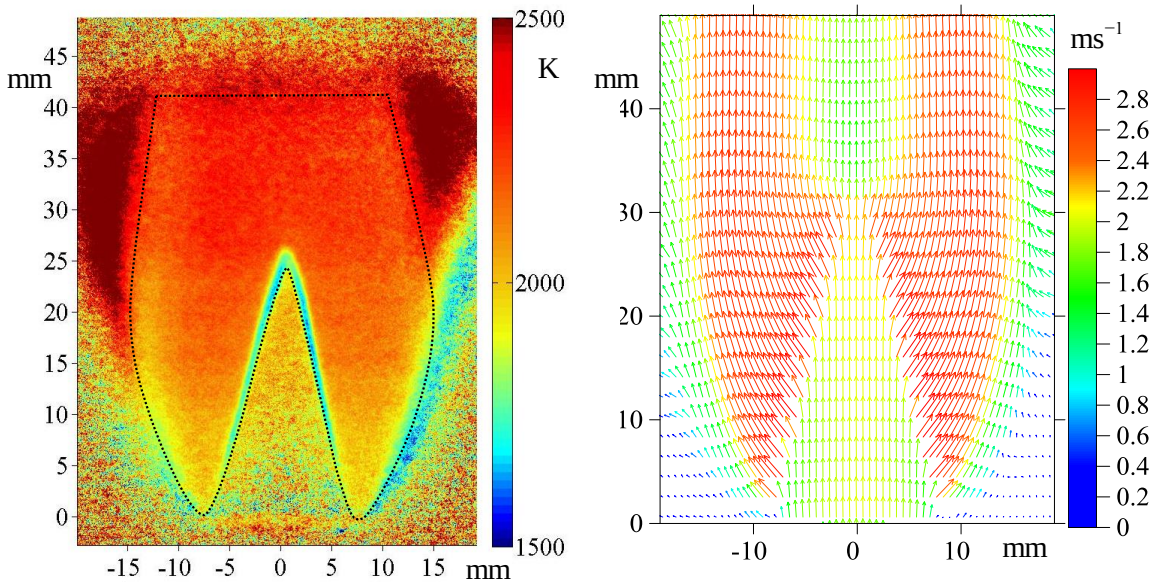

Figure 3. OH* PLIF and PIV results for unconfined conical flame (Φ = 0.9, Re = 1500)

A pair of lines $R_1(14)$ и $P_1(2)$ ($v' = 1 \leftarrow v'' = 0$, $A^2\Sigma^+ \leftarrow X^2\Pi$) was selected to evaluate gas temperature. The signal is shown in Figure 2. Figure 3 shows the results of PLIF and PIV measurements for the unconfined propane-air flame. The temperature of the products is in the range of

2000÷2200 K, whereas the adiabatic temperature of the propane-air flame (Φ = 0.9, 1 atm. and reactants temperature of 300 K), calculated using GRI-MECH 3.0 chemistry, is 2179 K. According to the analysis in [9], the uncertainty of the temperature measurement is expected to be roughly 10%.

3.2. Visualisation of impinging flames

Figure 4 shows the typical combustion regimes, which can be separate into two groups, namely, the seated flames, attached to the nozzle rim, and detached (lifted) flames, stabilized at a certain distance from the nozzle rim (similar flames were observed in [7]). The former type of the flames was observed for a wide range of H/d and Φ values. The lifted flames, stabilized near the impingement surface, were typical for fuel-rich mixtures and a wide range of H/d. Besides, lean lifted flames could exist near the impingement surface for $H/d = 1$ and 2, whereas unconfined flames were blown away for these conditions.

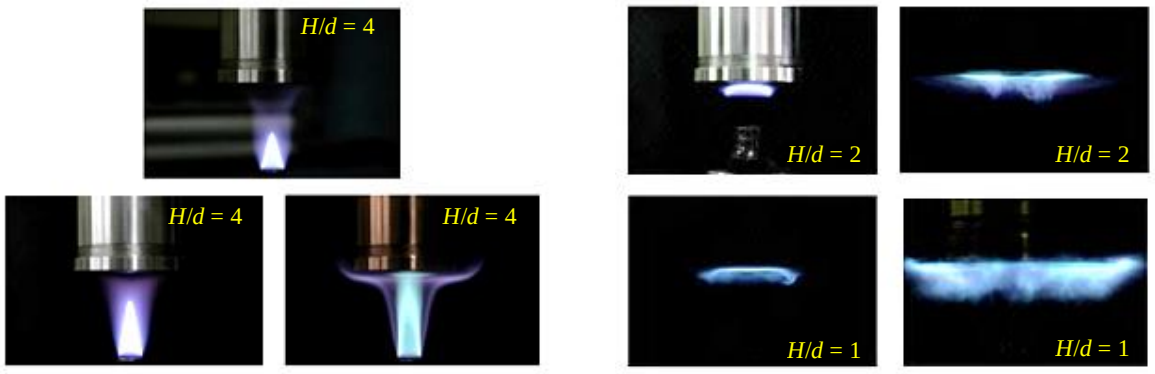

Figure 4. Photographs of seated (left) and detached (right) flame types

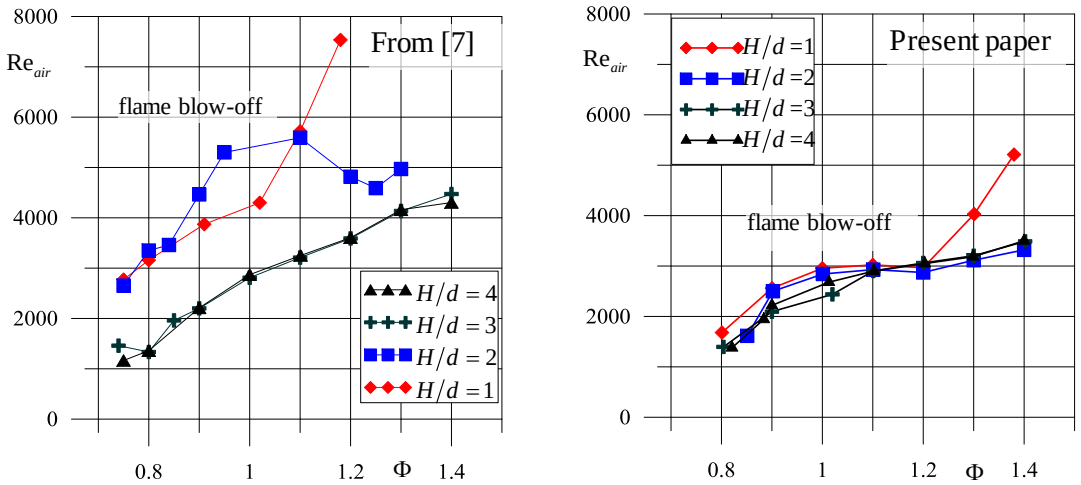

Figure 5. Blow-off curves for propane-air impinging flames for different nozzle-to-surface distances

Blow-off curves for different values of H/d are shown in Figure 5 on Re-Φ diagram. The Reynolds number is defined as $\mathrm{Re} = 4Q_{air}/\pi\nu_{air}d$, where Q_{air} and ν_{air} are the flowrate and kinematic viscosity of the air, respectively. The blow-off curves separate the conditions, for which the flame stabilized on the nozzle or near the impinging surface, from region of Re and Φ values for which the flame was blown away. For the cases of $H/d = 4$ and 8 the flame was attached to the nozzle rim before the blow-off (for the studied range of Φ between 0.8 and 1.4). For $H/d = 1$ and 2, mixture with Φ > 1.2 could burn as a detached (lifted) flame from the nozzle and stabilized near the impingement surface (see Figure 4).

Blow-off limits obtained in [7] for another nozzle with diameter of 18 mm are shown in Figure 5. Presence of the impingement surface for $H/d = 1$ and 2 provides extended range of Re and Φ for combustion without blow off.

3.3. PIV data for impinging flames

The average velocity fields measured for the reacting impinging jets (Φ = 0.9, Re_{air} = 1500) are shown in Figure 6. The bulk velocity of the mixture U_0 is approximately 1.6 ms^{-1}. The focus of this sub-section is on the impingement surface effect on the velocity field for the case of conical premixed flame. The data for the cases of H/d = 1, 2, 3, and 4 are presented. Except for H/d = 1, the flame had shape of a cone. The gas velocity increased downstream the flame front due to combustion and local gas density decrease. For the case H/d = 2 the cone top was located almost at the impingement surface. For the case H/d = 1 the flame shape was constricted by the obstacle. Important finding is a not intensive recirculation zone, present between the cone and the impingement surface for the case H/d = 4. Negative values of the axial velocity component are also detected for H/d = 3.

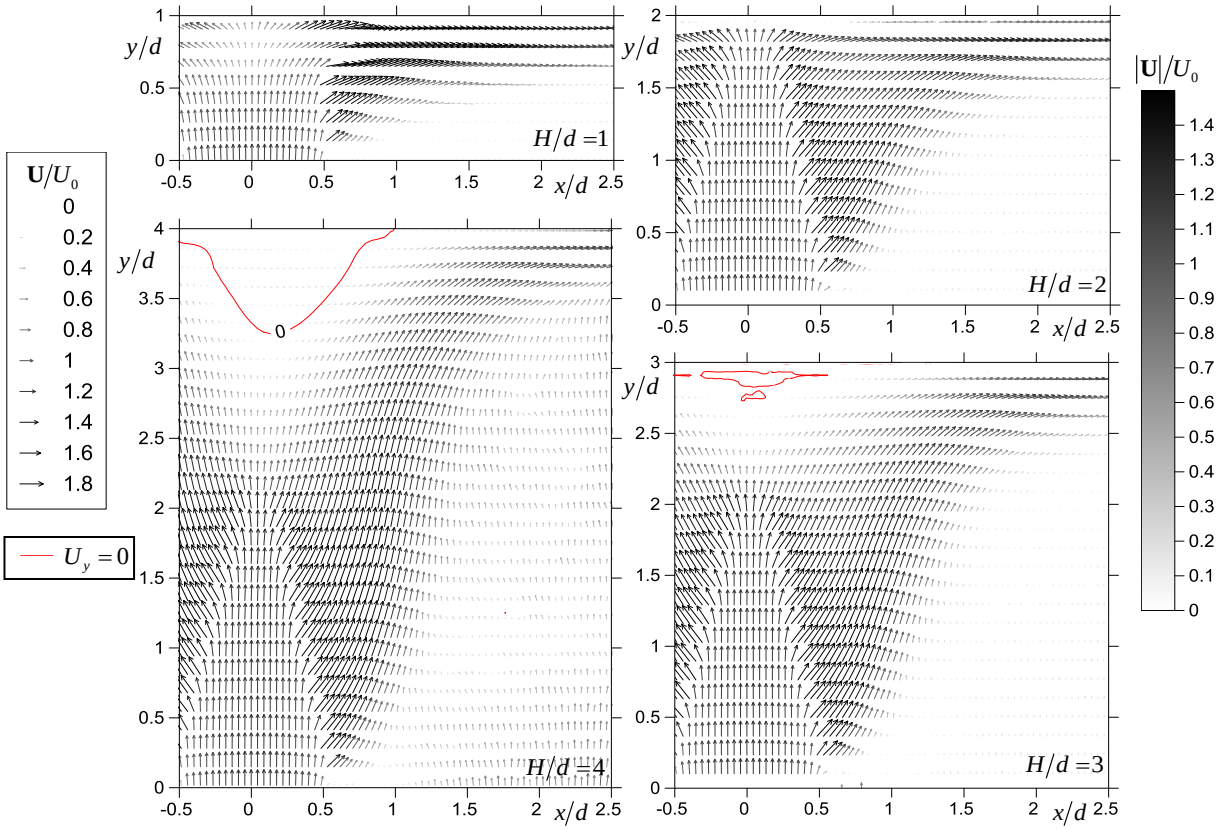

Figure 6. Mean velocity field for impinging propane-air flames (Φ = 0.9, Re_{air} = 1500) for different H/d

4. Conclusions

Flow structure of premixed propane-air impinging jet-flames was studied by planar optical tehcniques. Depending on values of Re and Φ and also on the way of the flame ignition, the observed flames corresponded to two different types. Flames, attached to the nozzle rim, were observed for a wide range of Φ and H/d. Fuel-rich mixture could also burn as a lifted flame. For H/d = 1 and 2 the impingement surface provided a wider range of Re and Φ (fuel-rich lifted flames with Φ > 1.2) for

combustion without blow-off. Moreover, lean lifted flames could also burn near the surface for these values of H/d.

The velocity field in the conical lean flames was measured by using PIV. The flows for H/d = 1, 2, 3, and 4 were compared. It was found that a weak recirculation zone was formed between the flame cone and the impingement surface for the case of H/d = 4. This finding is important because local recirculation provides a stagnation region which may reduce local heat transfer between the solid surface and combustion products.

5. Acknowledgments

This work was funded by Russian Science Foundation (grant No. 16-19-10566).

6. References

[1] Kataoka K, Suguro M, Degawa H, Maruo K, Mihata I 1987 The effect of surface renewal due to largescale eddies on jet impingement heat transfer. *Int. J. Heat Mass Transfer* **30** 559–67

[2] Meola C, de Luca L, Carlomagno G 1996 Influence of shear layer dynamics on impingement heat transfer. *Exp. Therm. Fluid Sci.* **13** 29–37

[3] Hadziabdic M, Hanjalic K 2008 Vortical structures and heat transfer in a round impinging jet. *J. Fluid Mech.* **596** 221–60

[4] Roux S, Fenot M, Lalizel G, Brizzi L, Dorignac E 2011 Experimental investigation of the flow field and heat transfer of an impinging jet under acoustic excitation. *Int. J. Heat Mass Transfer* **54** 3277-90

[5] Sakakibara J, Hishida K, Maeda M 1997 Vortex structure and heat transfer in the stagnation region of an impinging plane jet (simultaneous measurements of velocity and temperature fields by digital particle image velocimetry and laser-induced fluorescence. *Int. J. Heat Mass Transfer* **40** 3163–76

[6] Renard P-H, Thevenin D, Rolon J, Candel S 2000 Dynamics of flame/vortex interactions. *Progr. Energy Combust. Sci.* **26** 225-82

[7] Fernandes E, Leandro R 2006 Modeling and experimental validation of unsteady impinging flames. *Combust. Flame.* **146** 674–86

[8] Abdurakipov S, Dulin V, Markovich D, Hanjalic K 2013 Expanding the stability range of a lifted propane flame by resonant acoustic excitation. *Combust. Sci. Technol.* **185** 1644–66

[9] Devillers R., Bruneaux G., Schulz C 2008 Development of a two-line OH-laser induced fluorescence thermometry diagnostics strategy for gas-phase temperature measurements in engines. *Appl. Optics*, **47** 5871-85